ILAR Journal, 2016, Vol. 57, No. 1, 34–43

doi: 10.1093/ilar/ilw004
Article

Characterization of New Zealand White Rabbit Gut-Associated Lymphoid Tissues and Use as Viral Oncology Animal Model

Robyn A. Haines, Rebeccah A. Urbiztondo, Rashade A. H. Haynes II, Elaine Simpson, Stefan Niewiesk, and Michael D. Lairmore

Robyn A. Haines, DVM, was a PhD student; Rebeccah A. Urbiztondo, DVM, was a Master's student; Rashade A. H. Haynes, PhD, was a postdoctoral fellow; and Elaine Simpson, DVM, was a summer research student in the Department of Veterinary Biosciences at The Ohio State University in Columbus, Ohio. Stefan Niewiesk, PhD, DVM, is professor in the Department of Veterinary Biosciences at The Ohio State University is Columbus, Ohio. Michael D. Lairmore, DVM, PhD, is dean, in the School of Veterinary Medicine at the University of California, Davis in Davis, California.

Address correspondence and reprint requests to Stefan Niewiesk, PhD, DVM, College of Veterinary Medicine, The Ohio State University, 1900 Coffey Road, Columbus, OH 43210-1093 or email niewiesk.1@osu.edu.

Abstract

Rabbits have served as a valuable animal model for the pathogenesis of various human diseases, including those related to agents that gain entry through the gastrointestinal tract such as human T cell leukemia virus type 1. However, limited information is available regarding the spatial distribution and phenotypic characterization of major rabbit leukocyte populations in mucosa-associated lymphoid tissues. Herein, we describe the spatial distribution and phenotypic characterization of leukocytes from gut-associated lymphoid tissues (GALT) from 12-week-old New Zealand White rabbits. Our data indicate that rabbits have similar distribution of leukocyte subsets as humans, both in the GALT inductive and effector sites and in mesenteric lymph nodes, spleen, and peripheral blood. GALT inductive sites, including appendix, cecal tonsil, Peyer's patches, and ileocecal plaque, had variable B cell/T cell ratios (ranging from 4.0 to 0.8) with a predominance of CD4 T cells within the T cell population in all four tissues. Intraepithelial and lamina propria compartments contained mostly T cells, with CD4 T cells predominating in the lamina propria compartment and CD8 T cells predominating in the intraepithelial compartment. Mesenteric lymph node, peripheral blood, and splenic samples contained approximately equal percentages of B cells and T cells, with a high proportion of CD4 T cells compared with CD8 T cells. Collectively, our data indicate that New Zealand White rabbits are comparable with humans throughout their GALT and support future studies that use the rabbit model to study human gut-associated disease or infectious agents that gain entry by the oral route.

Key words: gut-associated lymphoid tissue (GALT); human T cell leukemia/lymphoma virus 1 (HTLV-1); intraepithelial lymphocytes; lamina propria lymphocytes; lymphoid tissue; rabbit; review; small intestine

Introduction

The rabbit has been used as an animal model to study infection through the mucosal route by human T cell leukemia/lymphoma virus 1 (HTLV-1) (Lairmore et al. 2005), *Mycobacterium tuberculosis* (Manabe et al. 2008), *Chlamydia pneumoniae* (Fong et al. 1997), rotavirus (Conner et al. 1988), and hepatitis E virus (Cheng et al. 2012). Rabbits are used extensively as a model for human HTLV-1 infection because of the ease and consistency of viral transmission and infection in this species. Infectivity in rabbits was first demonstrated in the mid-1980s by intravenous inoculation of a rabbit lymphocyte cell line, Ra-1, which had been infected with HTLV-1 through coculture with the HTLV-1–infected MT-2 cell line (Akagi et al. 1985; Miyoshi et al. 1985). Early studies in rabbits identified the routes of viral transmission (e.g., blood, semen, milk) (Hirose et al. 1988; Iwahara et al. 1990; Kataoka et al. 1990; Kotani et al. 1986; Uemura et al. 1986, 1987) and provided important clues as to the number of infected cells required for viral transmission (Kataoka et al. 1990). The rabbit model has provided important information about the immune responses during HTLV-1 infection. Early studies defined methods to detect the sequential development of antibodies against different viral proteins and HTLV-1 proviral DNA in infected tissues (Cockerell et al. 1990). Immunization of rabbits with synthetic peptides verified immunodominant epitopes of the viral envelope protein (Env) (Lal et al. 1991; Tanaka et al. 1991) and also defined regions of Env important for antibody-dependent cell-mediated cytotoxicity (Chen et al. 1991). Subsequently, it was demonstrated that peptide immunization with amino acids 190–199 of the Env protein could protect rabbits from HTLV-1 infection (Tanaka et al. 1994). More complex synthetic peptides, which use chimeric constructs that mimic native viral proteins, have also been generated and tested in the rabbit model (Conrad et al. 1995; Frangione-Beebe et al. 2000). Infectious molecular clones of HTLV-1 were first developed in the mid-1990s (Derse et al. 1995; Kimata et al. 1994; Zhao et al. 1995). These molecular clones were used to immortalize human peripheral blood mononuclear cells to create the ACH.2 cell line, which was then used to infect rabbits (Collins et al. 1996). It was demonstrated that the lethally irradiated ACH.2 cell line successfully establishes infection in the peripheral blood mononuclear cells of rabbits (Collins et al. 1996). Subsequently, HTLV-1 clones with mutations in the open reading frames encoding the HTLV-1 accessory proteins, p12, p13, and p30, were generated (Robek et al. 1998). These HTLV-1 clones were then inoculated into rabbits to demonstrate the necessity of these accessory proteins for establishment of infection and maintenance of proviral loads. HTLV-1 clones with selected mutations have been used to demonstrate the in vivo functional properties of HTLV-1 p12, p13, p30, Rex, and Env (Arnold et al. 2006; Bartoe et al. 2000; Collins et al. 1998; Hiraragi et al. 2006; Silverman et al. 2004, 2005).

In addition to being susceptible to a wide variety of human pathogens, the rabbit is in certain aspects advantageous compared with other animal models such as small rodents (e.g., mice and rats) and nonhuman primates. Rabbits are less expensive to house and easier to handle than nonhuman primates but are bigger than the traditionally used smaller laboratory animals and offer larger sample volumes for collection (e.g., blood and gut-associated lymphoid tissue [GALT]). GALT is of particular interest in HTLV-1 infection as a port of entry. Similar to other mucosa-associated lymphoid tissue (MALT) structures, GALT consists of inductive sites and effector sites (Brandtzaeg et al. 2008; Neutra et al. 2001). The most commonly identified inductive GALT sites are known as Peyer's patches but, depending on the species, may also include isolated lymphoid follicles, lymphoglandular complexes in the large intestine, and specialized inductive sites such as the appendix (Brandtzaeg and Pabst 2004; Nagler-Anderson 2001). Inductive sites within the GALT across all animal species consist of one or more follicles containing interspersed T cell–rich interfollicular areas with an overlying subepithelial dome of a single layer of columnar epithelial cells making up the follicle-associated epithelium (Brandtzaeg et al. 2008; Cesta 2006; Nagler-Anderson 2001). In the inductive sites of the GALT, antigens from the gut lumen are processed and presented to naïve T cells and B cells (Brandtzaeg and Pabst 2004). The effector sites of GALT are dispersed along the entire length of the gut and consist primarily of lymphocytes with a memory phenotype (Agace et al. 2000; Lefrancois et al. 1999). These include the intraepithelial lymphocytes (IELs), which are located between individual enterocytes in the mucosa, and the lamina propria lymphocytes (LPLs), which are located just beneath the intestinal epithelium in the lamina propria.

The only well-studied mucosa-associated lymphoid tissues in the rabbit are the nasal- and ocular-associated lymphoid tissues (Cain and Phillips 2008; Casteleyn et al. 2010; Nesburn et al. 2007), which are similar to those in humans. In addition to structural similarities, there are age-related changes in rabbit ocular-associated lymphoid tissues, which parallel changes described in humans (Cesta 2006).

Rabbits are true nonruminant herbivores and are considered hind gut fermenters. Their large cecum contains up to 40% of the intestinal contents and enables efficient digestion of a high-fiber diet (Kohles 2014). The rabbit cecum terminates in a smaller diameter tubular cecal "appendix" (Kohles 2014). Their proximal cecum has a prominent pouch called the sacculus rotundus, also known as the cecal tonsil (CT) because of its prominent lymphoid tissue. The ileocecal plaque is located adjacent to the CT at the proximal entrance of the cecal lumen. Both structures, the CT and the ileocecal plaque, contain abundant lymphoid follicles and are unique to the rabbit (Snipes 1978). In analyzing rabbit GALT, studies to date have focused on rabbit lymphoid microanatomy, M cell structure and function, and development of the primary antibody repertoire (Dasso et al. 2000; Gebert et al. 1992; Hanson and Lanning 2008; Lelouard et al. 2001). Limited reports have evaluated the T cell and B cell surface markers in rabbit mesenteric lymph nodes, spleen, and peripheral blood (Jeklova et al. 2007; Okita et al. 1995; Tokarz-Deptula and Deptula 2003, 2005). The objective of this study was the immunophenotypic characterization of major leukocyte populations and their distribution in rabbit GALT inductive and effector sites and its comparison with other secondary lymphoid tissues and the human GALT.

Materials and Methods

Animals

Tissues were collected from ten 12-week-old, female, specific pathogen–free (SPF) New Zealand White, HsdOkd:NZW (also called Ora:NZW) rabbits (Harlan; Oxford, MI). These SPF rabbits were reported test negative for rabbit hemorrhagic disease virus, myxomatosis virus, rotavirus, bordetella bronchiseptica, cilia-associated respiratory bacillus, *Clostridium piliforme, Corynebacterium kutscheri, Helicobacter spp, Klebsiella oxytoca, Klebsiella pneumoniae, Pasteurella multocida, Pseudomonas aeruginosa, Salmonella spp, Streptococcus pneumoniae, Streptococcus spp* group B beta, *Treponema cuniculi*, dermatophytes, *Toxoplasma spp*, *Encephalitozoon cuniculi*, ectoparasites, endoparasites, and enteric protozoa. Before euthanasia and tissue collection, rabbits were maintained

for 1 week, single housed in stainless steel caging. They received Teklad rabbit chow provided ad libitum and tap water in water bottles. All rabbits were premedicated with intramuscular injections of 10 mg/ml acepromazine (Vedco; St. Joseph, MO), 100 mg/ml ketamine (Fort Dodge Animal Health; Fort Dodge, IA) and 10 mg/ml butorphanol (Vedco) before injection of sodium thiopental (Abbott Laboratories; Chicago, IL) given by the auricular vein to accomplish complete anesthesia. Median thoracotomy was performed, and the pericardial sac was exposed and incised. Perfusion with 500 ml of heparinized saline was performed in the left ventricle with an 18-gauge needle. After saline perfusion, the ventral midline incision was extended to the pubis, and internal abdominal organs were exposed for sample collection. All tissue samples were collected from standardized locations after death. The animal use protocol was approved by the Institutional Animal Care and Use Committee of The Ohio State University.

Preparation of Lymphocytes from Tissues

Tissue samples from mediastinal lymph nodes, Peyer's patches (1–3 per animal), cecal tonsil, appendix, ileocecal plaque, and spleen were mechanically dissociated using sterile forceps and scissors. Dissociated tissue was then passed through 40-µm mesh sieves to obtain cell suspensions. Samples were centrifuged at 1400 RPM for 5 minutes at 37°C. Cell pellets were resuspended and filtered through a 40-µm nylon basket style sieve (BD Falcon; Franklin Lakes, NJ) and washed twice with phosphate-buffered saline. Lymphocytes from blood were separated over a Ficoll gradient by centrifugation for 30 minutes at 1800 RPM. Red blood cells were lysed by incubation of the cell pellet for 5 minutes in a hemolytic NH_4Cl buffer. After the lysis step, cells were washed twice to remove red blood cell debris. Remaining pellets were resuspended in 5 ml of RPMI/10% fetal calf serum (FCS) and counted with a hemocytometer.

Isolation of IELs

For the isolation of IELs, a protocol was adapted from Howard and colleagues (2005). Approximately 15 cm of duodenum were collected starting just distal to the pyloric antrum. All grossly visible lymphoid follicles were excised before processing. Intestinal sections were flushed twice with RPMI/10% FCS. Intestinal sections were then opened longitudinally and cut into 0.5 to 1 cm strips. The strips were placed into a 250-ml Erlenmeyer flask containing 40 ml of RPMI/10% FCS. Sections were stirred with a magnet at 900–1200 RPM for 45 minutes at 37°C on a hot plate. Subsequently, the remaining tissue was separated from the supernatant using a 40-µm sieve. The supernatant was centrifuged at 1200 RPM for 10 minutes at room temperature. After centrifugation, the supernatant was carefully discarded, and the pellet was resuspended in 40 ml of RPMI/10% FCS, strained through a 40-µm mesh sieve and centrifuged a second time. After the second centrifugation step, the supernatant was discarded, the pellet was resuspended in 5 ml of RPMI/10% FCS, and cells were counted.

Isolation of LPLs

After the removal of the IELs, the remaining intestinal tissue strips were resuspended in 40 ml of lymphocyte media containing 1 ml of Dispase II-neutral protease (1.9 units/ml; Roche Diagnostics; Indianapolis, IN). Tissues were then stirred at 700 to 800 RPM for 45 minutes at 37°C. After the first digestion step, the supernatant was collected by filtering through a 40-µm mesh sieve. This step was repeated to obtain additional lymphocytes.

Flow Cytometry

For flow cytometry, 1×10^5 cells were incubated with monoclonal antibody for 30 minutes at room temperature. Cells were subsequently washed twice with RPMI/10% FCS. In a second step, cells were then incubated with a fluorochrome-conjugated secondary antibody for 60 minutes. After washing, samples were fixed using 2% paraformaldehyde and analyzed (FACS Calibur, Immunocytometry Systems; BD Biosciences, Sparks, MD, USA). Antibodies and manufacturer information are summarized in Table 1.

Histological Tissue Survey

In the stomach, cecum, and colon of most animals, lymphoid aggregates were not evident grossly. The following tissues were obtained for histological analysis: palatine tonsil, stomach (fundus, body, and pyloric region), duodenum and adjacent pancreas, three sections of jejunum, ileum, and jejunal and ileal Peyer's patches (located approximately every 15–20 cm along the entire length of the small intestine), ileocecal plaque, cecal tonsil (sacculus rotundus), appendix, cecum, colon (40 cm from cecum), mesenteric lymph nodes, spleen (midsection), and liver (left lateral lobe). Tissues were fixed in 10% neutral buffered formalin for 48 hours and embedded in paraffin; 5-µm thick sections were cut from paraffin-embedded tissue, deparaffinized, and stained with hematoxylin and eosin.

Immunohistochemistry

Frozen Tissue Sections

Frozen tissue sections were obtained from nine different locations: duodenum, mid-jejunum, ileum, Peyer's patch, appendix,

Table 1 Immunochemical reagents used for cell identification by flow cytometry and immunohistochemistry

Cell lineage	Marker	Antigen source	Antibody host species	Antibody clone number	Antibody vendor	Application
T lymphocyte	CD4	Rabbit	Mouse	KEN-4	Antigenix	FC
T lymphocyte	CD8	Rabbit	Mouse	C7	Antigenix	FC
Lymphocytes	CD45	Rabbit	Mouse	L12	Antigenix	FC
B cell	IgM	Rabbit	Mouse	NRBM	Antigenix	FC
Macrophages	CD11b	Rabbit	Mouse	198	Antigenix	FC
Proliferating cells	Ki-67	Human	Mouse	PP-67	Thermo Scientific	FC
T lymphocytes (mouse)	CD3	Human	Rabbit		Dako Catalogue No. A0452	IHC
B lymphocytes (human)	CD79a	Human	Mouse	HM57	Dako Catalogue No. M7051	IHC

CD, cluster of differentiation; FC, flow cytometry; Ig, immunoglobulin; IHC, immunohistochemistry.

cecal tonsil, ileocecal plaque, spleen, and mesenteric lymph node. All frozen tissue specimens were taken immediately adjacent to the formalin-fixed specimens with the exception of Peyer's patches, which were collected as individual specimens. Four to eight serial frozen sections (10 µm) were obtained from each of the tissues and placed on glass slides. Slides were fixed in acetone for 5 minutes, then rinsed with water to remove all optimal cutting temperature compound. The slides were then rinsed with wash buffer (Dako; Carpinteria, CA) and placed in 0.3% hydrogen peroxide (diluted with Dako wash buffer) for 5 minutes, then rinsed again with wash buffer. Each slide was dried and then blocked for 10 minutes with serum-free protein block (Dako). Primary antibodies were incubated for 30 minutes at the indicated dilutions (Dako antibody diluent). Negative control slides were incubated with wash buffer only. Slides were rinsed twice with wash buffer, dried, and then incubated with Biotin Block for 30 minutes (Dako buffer with 5% milk). Slides were again rinsed twice with wash buffer and incubated for 30 minutes with the secondary antibody. Slides were washed twice with wash buffer and incubated with Avidin/biotin complex (Dako) for 30 minutes. Slides were washed twice with wash buffer and incubated with diaminobenzidine (DAB) (Dako) for 1 minute. Slides were rinsed in water to stop the reaction, counterstained with hematoxylin, fixed with ethanol gradients and xylene, allowed to dry, and then covered with glass cover slips. Antibodies and manufacturer information are summarized in Table 1.

Formalin-Fixed, Paraffin-Embedded Tissue

Tissue sections prepared from paraffin-embedded blocks were deparaffinized in xylene. Targeted retrieval solution (Dako) was applied to each slide before heating to 125° Celsius, then cooling to 90° Celsius for 10 seconds, and finally cooling to room temperature for 10 minutes. The slides were then rinsed with wash buffer (Dako) and placed in 3% hydrogen peroxide (diluted with Dako wash buffer) for 10 minutes, then rinsed with distilled water. Slides were rinsed again with wash buffer and then blocked for 10 minutes with serum-free protein block (Dako). Unconjugated primary antibodies were incubated for 30 minutes at the indicated dilutions (Dako antibody diluent). Slides were rinsed twice with wash buffer, dried, and then incubated with blocking solution for 30 minutes (Dako buffer with 5% milk). Slides were again rinsed twice with wash buffer and incubated for 30 minutes with the horseradish-peroxidase-conjugated secondary antibody. Slides were washed twice with wash buffer and incubated with Avidin/biotin complex (Dako) for 30 minutes. Slides were washed twice with wash buffer and incubated with DAB (Dako) for 1 minute. Slides were rinsed in water to stop the reaction, counterstained with hematoxylin, and fixed with ethanol gradients and xylene. After drying, the slides were covered with coverslips. Antibodies and manufacturer information are summarized in Table 1.

Area Measurements

Formalin-fixed, paraffin-embedded tissue sections were stained with antibody and scanned (Aperio ScanScope XT; LeicaBiosystems, Buffalo Grove, IL, USA). The cross-sectional areas of the Peyer's patch, ileocecal plaque, cecal tonsil, and appendix were measured using the pen tool in Aperio ImageScope Viewer. The follicular region and germinal center (proliferation zone) areas were outlined and calculated as a percentage of the total cross-sectional area as described in Dasso and colleagues 2000. The germinal center was defined as the area staining with Ki-67 (Dasso et al. 2000).

Positive Pixel Count Analysis

Slides were scanned (Aperio ScanScope XT) and analyzed by comparing positive pixel counts (Aperio Technologies). For mesenteric lymph node and spleen, the entire cross-section was included. For the Peyer's patch, ileocecal plaque, cecal tonsil, and appendix, the largest area of intact tissue was included. Lines were drawn between the interfollicular T cell zones to include entire B cell follicles, and oblique sections were avoided. Each slide was visually inspected to ensure specificity and sensitivity of antibody staining. Additionally, after positive pixel count analysis was run, analyzed slides were examined to confirm that positively identified pixels were consistent with lymphocyte staining and not background staining. Percentages were calculated as the total number of positive pixels divided by the total number of pixels.

Statistics

Log transformation was used to stabilize variance and to ensure model assumptions on normality were met. The ratios between CD4 and CD8 T cells and between B cells and T were tested among tissue types by a linear mixed-effects model. To compare positive pixel count versus area measurements on formalin-fixed slides, Pearson's correlation coefficient was calculated.

Results

Histological Tissue Survey

To define in more detail the rabbit GALT, we sampled the palatine tonsil, stomach, duodenum and adjacent pancreas, jejunum, ileum, cecum, colon, liver, Peyer's patches, ileocecal plaque, cecal tonsil (saculus rotundus), appendix, mesenteric lymph nodes, and spleen for histological analysis. Diffuse lymphocyte populations were present throughout the small and large intestine within the lamina propria (LPLs) and within the epithelium (IELs). In some animals, lymphoid aggregates were found in the stomach body (1 of 10 rabbits) and pylorus (2 of 10), cecum (2 of 10), or colon (2 of 10). A lymphoid aggregate was defined as a discrete population of lymphocytes that did not contain a germinal center. The majority of organized GALT, however, was present within the Peyer's patches, appendix, and cecal tonsil.

Lymphocyte Subset Quantification by Flow Cytometry

The GALT is usually divided into inductive (Peyer's patches, appendix, cecal tonsil, and ileocecal plaque) and effector sites (LPLs and IELs). To quantify lymphocyte subpopulations, we purified lymphocytes from these sites and compared them with lymphocytes from the blood, the mesenteric lymph node, and the spleen. These lymphocytes were stained with the common lymphocyte marker (CD45), T cell markers (CD4 and CD8), B cell marker (IgM) and a macrophage marker (CD11b) (Figure 1). In the mesenteric lymph node and the effector sites (LPLs and IELs), the percentage of T cells was higher than the percentage of B cells. In the spleen, B cells were the majority of all cells. In the inductive sites, Peyer's patches, cecal tonsil, and ileocecal plaque displayed a balanced percentage of T cells and B cells, whereas in the appendix B cells predominated (Table 2). The CD4/CD8 T cell ratios in the GALT inductive sites were 9.0 in the ileocecal plaque, 8.0 in the cecal tonsil, 7.0 in the Peyer's patches, and 3.5 in the appendix (Table 3). Interestingly, these ratios were significantly higher than the ratios reported in cats, rhesus macaques, rats, and humans (Howard et al. 2005; Jeklova et al. 2007; Kang et al. 1993; Lefrancois et al. 1999, 2001). In contrast, the CD4/CD8 T cell ratio in LPLs and IELs was more balanced (Table 3).

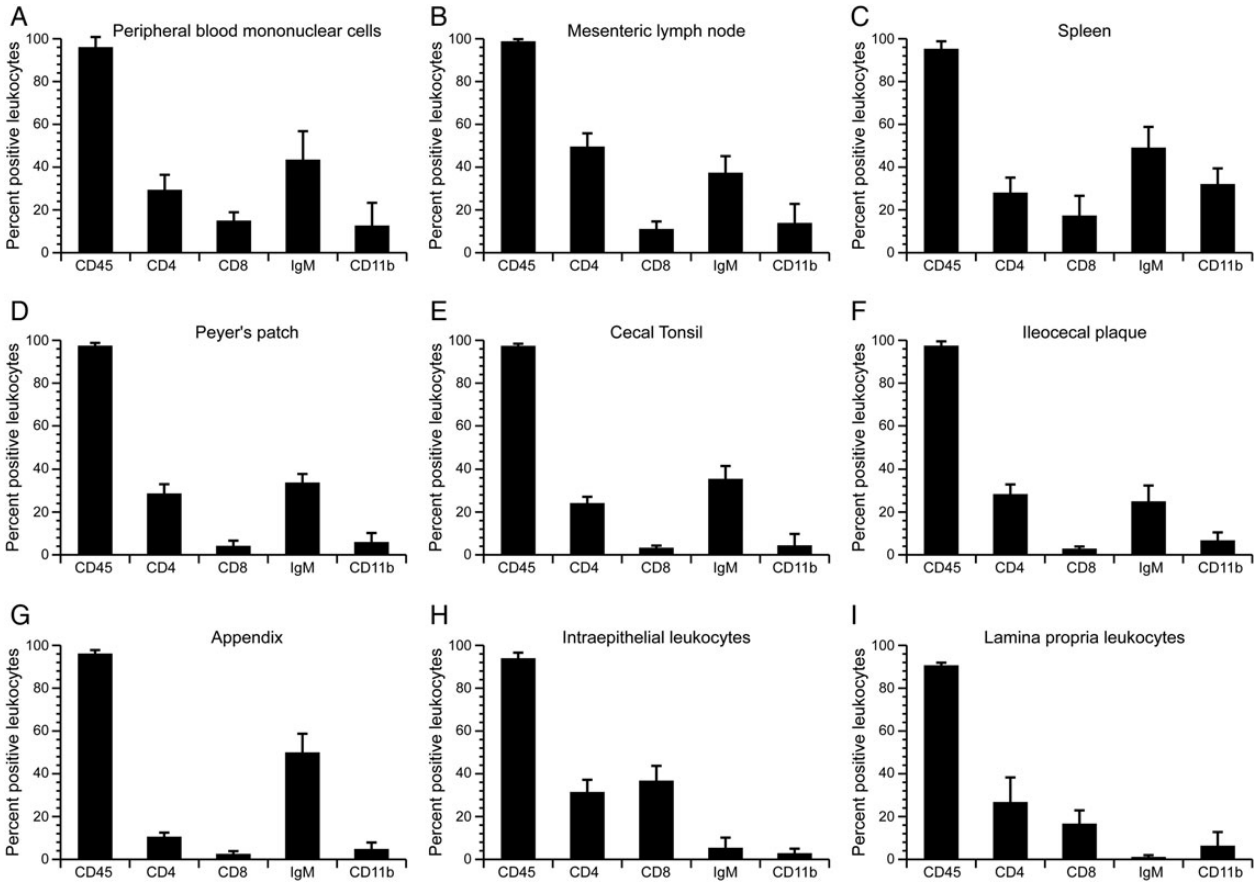

Figure 1 Analysis of lymphocyte populations from different lymphoid organs in the rabbit gastrointesional tract by flow cytometry. The percentages of lymphocytes expressing CD45, CD4, CD8, IgM, and CD11b are shown for 9 tissues. (A) Peripheral blood mononuclear cells. (B) Mesenteric lymph node. (C) Spleen. (D) Peyer's patch. (E) Cecal tonsil. (F) Ileocecal plaque. (G) Appendix. (H) Intraepithelial lymphocytes. (I) Laminar propria lymphocytes. Means and standard deviations were calculated based on results obtained from ten 12-week-old New Zealand White rabbits.

Table 2 Distribution of B and T cell subsets in MALT and systemic lymphoid tissues

Tissues	B cell (% positive cells ± SD)	T cell (% positive cells ± SD)	Ratio of B cells to T cells
Mucosa-associated Lymphoid tissues			
Appendix	50 ± 9	13 ± 2	4.0
Cecal tonsil	36 ± 6	27 ± 3	1.3
Peyer's patch	34 ± 4	33 ± 4	1.0
Ileocecal plaque	25 ± 7	32 ± 4	0.8
Intraepithelial leukocytes	5 ± 4	69 ± 12	0.1
Lamina propria leukocytes	1 ± 1	56 ± 11	0.01
Systemic tissues			
Spleen	49 ± 10	37 ± 10	1.3
Peripheral blood	44 ± 13	45 ± 7	1.0
Mesenteric lymph node	37 ± 8	56 ± 9	0.7

Table 3 Distribution of CD4 and CD8 T cells in MALT and systemic lymphoid tissues

Tissues	CD4 (% positive cells ± SD)	CD8 (% positive cells ± SD)	Ratio of CD4 T cells to CD8 T cells
Mucosa-associated lymphoid tissues			
Ileocecal plaque	28 ± 5	3 ± 1	9.0
Cecal tonsil	24 ± 3	3 ±	8.0
Peyer's patch	29 ± 4	4 ± 2	7.0
Appendix	11 ± 2	3 ± 1	3.5
Lamina propria leukocytes	27 ± 12	17 ± 6	1.6
Intraepithelial leukocytes	31 ± 6	37 ± 7	0.8
Systemic tissues			
Mesenteric lymph node	50 ± 6	11 ± 3	4.5
Peripheral blood	29 ± 7	15 ± 4	2.0
Spleen	28 ± 7	17 ± 9	1.6

Immunohistochemistry and Lymphocyte Subset Quantification

To define not just the number of lymphocytes but the size of the respective T cell and B cell areas in lymphoid tissue, immunohistochemical stainings for B cells (CD79a) and for T cells (CD3) were performed. The morphology of the Peyer's patches, appendix, cecal tonsil, and ileocecal plaque was similar in that they contained prominent B cell subepithelial domes and follicles containing germinal centers surrounded by T cell–rich zones, with smaller numbers of T cells within B cell regions, the mucosa, and submucosa (Figures 2–5). Using a morphometric

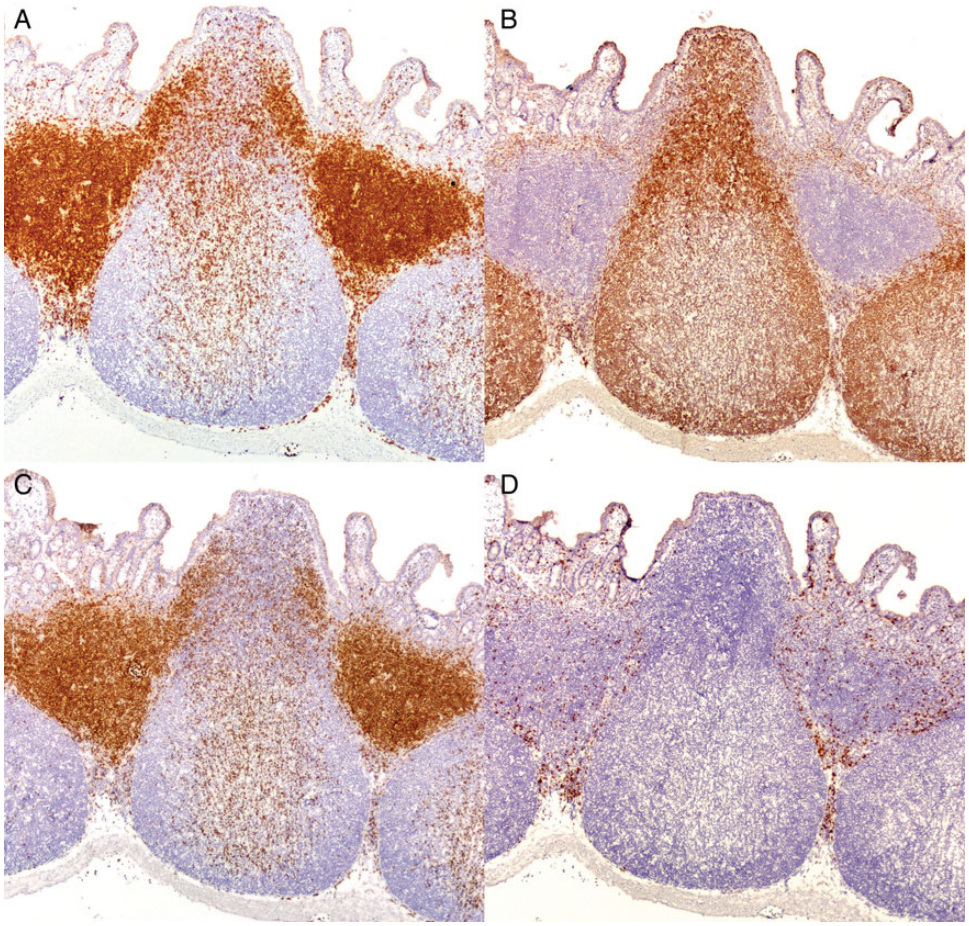

Figure 2 Lymphocyte distribution in the ileocecal plaque of the rabbit (original magnification 100x). Immunohistochemistry of the ileocecal plaque with antibodies against (A) CD3, (B) CD79a, (C) CD4, and (D) CD8. The structure of the ileocecal plaque is similar to that of a Peyer's patch. (A) Anti-CD3 stains T cell–rich parafollicular regions as well as scattered cells throughout B cell–predominant follicles, the submucosa, and mucosa. (B) Inductive sites are flask shaped, consisting of CD79a positive follicles under a narrower CD79a positive subepithelial dome region. There is a predominance of (C) CD4 cells to (D) CD8 cells in all GALT effector sites.

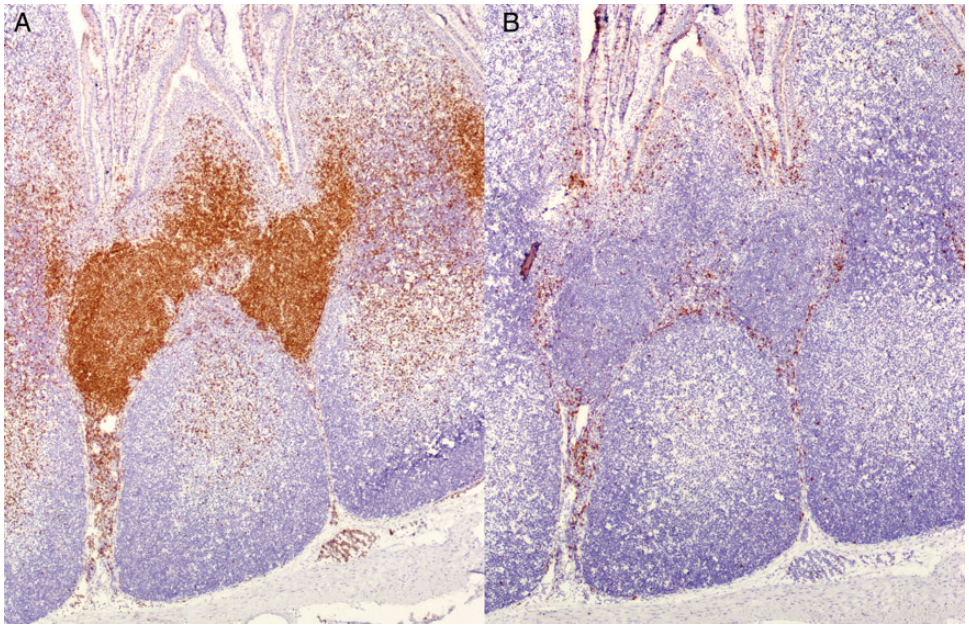

Figure 3 CD4 and CD8 T cell distribution in cecal tonsil of the rabbit (original magnification 100x). Immunohistochemistry of the cecal tonsil with antibodies against (A) CD4 and (B) CD8 T cells. (A) Within T cell parafollicular zones, the majority of the cells are CD4 positive. T cell zones contain smaller numbers of (B) CD8-positive cells compared with (A) CD4-positive cells.

Figure 4 Quantitative area analysis for Ki-67 in the Peyer's patch of the rabbit (original magnification 100x). Immunohistochemistry of the Peyer's patch stained with antibody against Ki-67. Positive staining identifies the germinal center. Formalin-fixed, paraffin-embedded tissue sections were stained with antibody and scanned (Aperio ScanScope XT; LeicaBiosystems). The cross-sectional area of the Peyer's patch, ileocecal plaque, cecal tonsil, and appendix were measured using the pen tool in Aperio ImageScope Viewer. The follicular region and germinal center (proliferation zone, green line) areas were outlined and calculated as a percentage of the total cross-sectional area (yellow line), as described in Dasso and colleagues 2000). The germinal center was defined as the area staining with Ki-67 (Dasso et al. 2000).

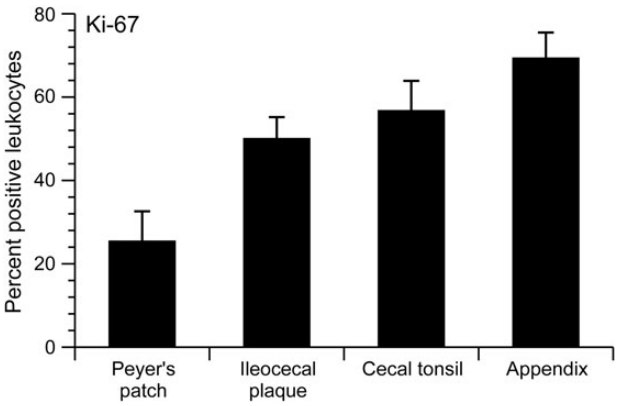

Figure 5 Comparison of germinal centers within inductive sites. Based on the percentage of positive Ki-67 lymphocytes in the follicular region area, the Peyer's patches, ileocecal plaque, cecal tonsil, and appendix were compared. The Peyer's patches have the smalllest percentage of germinal center tissue of all inductive sites.

method, the percentage of the areas staining positive for B cells or T cells was determined as the percentage of the total cross-section. Based on this analysis, the ratio of B cell to T cell areas was calculated for each tissue. The B cell/T cell area ratio was similar in the Peyer's patches and ileocecal plaques (2.2 and 2.1), increased in the cecal tonsil (3.9), and was highest in the appendix (7.3). However, histological examination of the sections revealed a significant proportion of T lymphocytes within B cell follicular areas that was not counted by the area quantification method. To overcome this limitation, we used a positive pixel count method. Positively staining cells were quantified by the numbers of positive pixels for each of the immunohistochemical markers (CD79a and CD3) compared with the total number of pixels in a standardized area. Overall, the results of the area quantification and the positive pixel method correlated well with each other (Table 4). The highest correlations were found for the T cell areas and the B cell/T cell ratios (Pearson's correlation coefficients of 0.94 and 0.89, respectively) with a slightly lower correlation between the measurements of the B cell area (Pearson's correlation coefficient of 0.50; p value = 0.0071). Both methods demonstrated a high B cell/T cell ratio in the appendix with low values for the Peyer's patches, cecal tonsil, and ileocecal plaque.

CD4 and CD8 T Cell Populations

To characterize T cell populations, positive pixel count analysis was performed on frozen tissue sections stained with antibodies against CD4 and CD8. CD4 T cells exceeded CD8 T cells in all areas examined. The CD4 T cell/CD8T cell ratios were 2.0 in the appendix, 2.6 in the Peyer's patches, 3.7 in the cecal tonsil, and 3.6 in the ileocecal plaque. The mesenteric lymph node had a ratio of 2.5, and the spleen had a ratio of 1.8. Statistical analysis of all cell populations (B cells, CD4 T cells, and CD8 T cells) in these tissues indicate that the T cell–dominant Peyer's patches, cecal tonsil, and ileocecal plaque are most like the T cell–dominant mesenteric lymph node and that the B cell–dominant appendix shares more similarities with the B cell–dominant spleen.

Germinal Center Formation in Inductive Sites

The morphometric analysis does not correlate directly with function or activity of lymphocytes. However, it has been shown previously that germinal center activity correlates with B cell proliferation and that Ki-67 staining identifies these areas (Dasso et al. 2000). Ki-67 staining was measured by the area quantification method and expressed as the ratio of area of proliferation/follicular (B cell) region (Figure 5). All inductive tissues had germinal center activity. However, among all of the tissues examined, the Peyer's patches had significantly smaller germinal center areas (2–4-fold difference).

Discussion

As a model for gastrointestinal disease, rabbits share many similarities to humans within their upper gastrointestinal tract (stomach, duodenum, and jejunum) and are considered to be a highly relevant animal model for studies in this anatomic region (Kararli 1995). In addition, the stomach and duodenum in both humans and rabbits have a similar pH and comparable populations of commensal organisms (Kararli 1995). However, the study of complex early mucosal events in the gut requires understanding of its MALT, the GALT, and its inductive and effector regions. The inductive regions are organized collections of lymphocytes separated from the surface by a specialized follicle-associated epithelium containing specialized M cells (Rumbo et al. 2004). M cells and dendritic cells sample antigens from the lumen without processing them and present them to naïve lymphocytes residing underneath (Miller et al. 2007). These lymphocytes can recognize the antigen and traffic to nearby mesenteric lymph nodes. Previous studies with rabbits have shown many similarities between the MALT of rabbits and humans. Specific to the GALT, numerous comparisons have been

Table 4 Comparison of B cell and T cell area measurement by the area quantification and positive pixel count analysis

Tissues	Area quantification (% positive area/total area)			Positive pixel count analysis (% positive pixels/total pixels)		
	B cell area (CD79a)	T cell area (CD3)	Ratio of B cell to T cell area	B cell area (CD79a)	T cell area (CD3)	Ratio of B cell to T cell area
Ileocecal plaque	53 ± 5	24 ± 7	2.1	44 ± 9	25 ± 6	1.9
Cecal tonsil	55 ± 3	14 ± 2	3.9	43 ± 4	17 ± 3	2.6
Peyer's patch	44 ± 18	22 ± 10	2.2	42 ± 4	22 ± 4	2
Appendix	70 ± 5	10 ± 1	7.3	52 ± 9	9 ± 1	5.6

made between the rabbit and human appendix based on B lymphocyte populations and antibody development (Pospisil and Mage 1998). The identification of M cells and ultrastructural comparisons of the rabbit palatine tonsils and the Peyer's patches revealed additional similarities (Nishikawa and Takagi 1988). However, there is a gap in the knowledge of T lymphocyte populations within rabbit GALT structures. Our data indicate that the majority of the GALT in the rabbit is within the Peyer's patches, ileocecal plaque, cecal tonsil, and appendix. These four tissues all represent GALT inductive sites. The palatine tonsil also represents an inductive site in the rabbit. This is the only oral tonsil present in the rabbit, and it represents a minimal amount of lymphoid tissue (Casteleyn et al. 2011; Nishikawa and Takagi 1988). Other lymphoid aggregates in the stomach, cecum, and colon were minimal in these SPF rabbits and were not evident grossly. Similar to other species and previous reports in rabbits, intraepithelial and lamina propria lymphocytes (representing GALT effector sites) were present throughout the length of the gastrointestinal tract. Our quantitative analysis of the major GALT inductive sites confirms the predominance of CD4 T cells to CD8 T cells as reported in other species, including humans (Haley 2003; Jung et al. 2010). These results were supported by flow cytometry analysis of single cell preparation from the same tissues. The cecal tonsil had a statistically different ratio of CD4 to CD8 T cells when compared with the appendix and spleen (p values of 0.0108 and 0.0466, respectively) but was similar to the Peyer's patches, ileocecal plaque, and mesenteric lymph node. The rabbit has two unique lymphoid GALT structures, the cecal tonsil (or sacculus rotundus) and the ileocecal plaque. These structures have both been described as modified Peyer's patches (Kararli 1995), and one report compares the cecal tonsil to the human appendix (Snipes 1978). However, this designation appears to be based only on morphological features, and our results show that the distribution of lymphocyte populations in the cecal tonsil, as measured by multiple methods, is not similar to that in the human appendix. Although the cecal tonsil's lymphocyte distribution is most like the Peyer's patches and ileocecal plaque, there are distinct differences in B cell and T cell ratios that may make this structure unique. Based on the same analysis, the ileocecal plaque is essentially a Peyer's patch with a specific, identifiable location. Although the ileocecal plaque has a specific designation in rabbits, the presence of a Peyer's patch at the ileocecal orifice is common among many mammalian species, including humans (Haley 2003; Kararli 1995). Using the area quantification method, we quantified germinal centers as the percentage of area stained by Ki-67 in the Peyer's patches, cecal tonsils, and ileocecal plaques. Interestingly, despite the similarities in the B cell/T cell ratios in the Peyer's patches, cecal tonsil, and ileocecal plaque, the Peyer's patches in these young adult SPF animals had 2–4-fold smaller germinal centers compared with the other inductive sites assessed. Overall numbers of Peyer's patches in humans are influenced by age and are expected to peak at 15–25 years and then to decrease (Jung et al. 2010). Similarly, Peyer's patches in other species are expected to vary in size and numbers with age and exposure to intraluminal antigens. In addition, the overall size and numbers of follicles in Peyer's patches increase distally in the gut (Haley 2003; Kararli 1995). Age and microbial status of study animals is a relevant consideration for studies of gut conditions, and the germinal center size in this study is likely to have been influenced by the relatively young age and clean microbial status of these rabbits.

This study illustrates many similarities between rabbit GALT and human GALT with regard to B cell, CD4 T cell, and CD8 T cell populations. Future studies should evaluate the role of γδ-T cells in the rabbit GALT. Collectively, our data show strong similarities in the T lymphocyte populations of the major GALT inductive tissues with a predominance of CD4 T cells to CD8 T cells, similar to humans. Rabbit Peyer's patches, ileocecal plaque, and cecal tonsil are predominantly T cell structures similar to their mesenteric lymph node, and the appendix (like their spleen) is a predominantly B cell structure, similar to the human appendix and spleen. The study identifies the major inductive sites in rabbit GALT, which include the Peyer's patches, cecal tonsil, cecal appendix, and ileocecal plaque. Although the ileocecal plaque is considered a structure unique to the rabbit, our analysis of lymphocyte populations identifies it essentially as a site-specific Peyer's patch. We have further validated two methods for quantifying immunohistochemstry, positive pixel count and area analysis, and provided reference ranges for future studies. This characterization of similarities between rabbit and human GALT confirms and enhances the utility of the rabbit for the study of gut-associated disease and infectious agents that gain entry by the oral route.

Acknowledgments

This work was supported by a National Cancer Institute Program Grant P01CA100730 awarded to M. Lairmore. The authors thank T. Vojt for illustrations.

References

Agace WW, Roberts AI, Wu L, Greineder C, Ebert EC, Parker CM. 2000. Human intestinal lamina propria and intraepithelial lymphocytes express receptors specific for chemokines induced by inflammation. Eur J Immunol 30:819–826.

Akagi T, Takeda I, Oka T, Ohtsuki Y, Yano S, Miyoshi I. 1985. Experimental infection of rabbits with human T-cell leukemia virus type 1. Jpn J Cancer Res 76:86–94.

Arnold J, Yamamoto B, Li M, Phipps AJ, Younis I, Lairmore MD, Green PL. 2006. Enhancement of infectivity and persistence in vivo by HBZ, a natural antisense coded protein of HTLV-1. Blood 107:3976–3982.

Bartoe JT, Albrecht B, Collins ND, Robek MD, Ratner L, Green PL, Lairmore MD. 2000. Functional role of pX open reading

frame II of human T-lymphotropic virus type 1 in maintenance of viral loads in vivo. J Virol 74:1094–1100.
Brandtzaeg P, Kiyono H, Pabst R, Russell MW. 2008. Terminology: Nomenclature of mucosa-associated lymphoid tissue. Mucosal Immunol 1:31–37.
Brandtzaeg P, Pabst R. 2004. Let's go mucosal: Communication on slippery ground. Trends Immunol 25:570–577.
Cain C, Phillips TE. 2008. Developmental changes in conjunctiva-associated lymphoid tissue of the rabbit. Invest Ophthalmol Vis Sci 49:644–649.
Casteleyn C, Breugelmans S, Simoens P, Van den Broeck W. 2011. The tonsils revisited: Review of the anatomical localization and histological characteristics of the tonsils of domestic and laboratory animals. Clin Dev Immunol 2011:472460.
Casteleyn C, Broos AM, Simoens P, Van den Broeck W. 2010. NALT (nasal cavity-associated lymphoid tissue) in the rabbit. Vet Immunol Immunopathol 133:212–218.
Cesta MF. 2006. Normal structure, function, and histology of mucosa-associated lymphoid tissue. Toxicol Pathol 34:599–608.
Chen YM, Zhang XQ, Dahl CE, Samuel KP, Schooley RT, Essex M, Papas TS. 1991. Delineation of type-specific regions on the envelope glycoproteins of human T cell leukemia viruses. J Immunol 147:2368–2376.
Cheng X, Wang S, Dai X, Shi C, Wen Y, Zhu M, Zhan S, Meng J. 2012. Rabbit as a novel animal model for hepatitis E virus infection and vaccine evaluation. PLoS One 7:e51616.
Cockerell GL, Lairmore M, De B, Rovnak J, Hartley TM, Miyoshi I. 1990. Persistent infection of rabbits with HTLV-I: Patterns of anti-viral antibody reactivity and detection of virus by gene amplification. Int J Cancer 45:127–130.
Collins ND, Newbound GC, Albrecht B, Beard JL, Ratner L, Lairmore MD. 1998. Selective ablation of human T-cell lymphotropic virus type 1 p12I reduces viral infectivity in vivo. Blood 91:4701–4707.
Collins ND, Newbound GC, Ratner L, Lairmore MD. 1996. In vitro CD4+ lymphocyte transformation and infection in a rabbit model with a molecular clone of human T-cell lymphotrophic virus type 1. J Virol 70:7241–7246.
Conner ME, Estes MK, Graham DY. 1988. Rabbit model of rotavirus infection. J Virol 62:1625–1633.
Conrad SF, Byeon IJ, DiGeorge AM, Lairmore MD, Tsai MD, Kaumaya PT. 1995. Immunogenicity and conformational properties of an N-linked glycosylated peptide epitope of human T-lymphotropic virus type 1 (HTLV-I). Biomed Pept Proteins Nucleic Acids 1:83–92.
Dasso JF, Obiakor H, Bach H, Anderson AO, Mage RG. 2000. A morphological and immunohistological study of the human and rabbit appendix for comparison with the avian bursa. Dev Comp Immunol 24:797–814.
Derse D, Mikovits J, Polianova M, Felber BK, Ruscetti F. 1995. Virions released from cells transfected with a molecular clone of human T-cell leukemia virus type I give rise to primary and secondary infections of T cells. J Virol 69:1907–1912.
Fong IW, Chiu B, Viira E, Fong MW, Jang D, Mahony J. 1997. Rabbit model for Chlamydia pneumoniae infection. J Clin Microbiol 35:48–52.
Frangione-Beebe M, Albrecht B, Dakappagari N, Rose RT, Brooks CL, Schwendeman SP, Lairmore MD, Kaumaya PT. 2000. Enhanced immunogenicity of a conformational epitope of human T-lymphotropic virus type 1 using a novel chimeric peptide. Vaccine 19:1068–81.
Gebert A, Hach G, Bartels H. 1992. Co-localization of vimentin and cytokeratins in M-cells of rabbit gut-associated lymphoid tissue (GALT). Cell Tissue Res 269:331–340.
Haley PJ. 2003. Species differences in the structure and function of the immune system. Toxicology 188:49–71.
Hanson NB, Lanning DK. 2008. Microbial induction of B and T cell areas in rabbit appendix. Dev Comp Immunol 32:980–991.
Hiraragi H, Kim SJ, Phipps AJ, Silic-Benussi M, Ciminale V, Ratner L, Green PL, Lairmore MD. 2006. Human T-lymphotropic virus type 1 mitochondrion-localizing protein p13(II) is required for viral infectivity in vivo. J Virol 80:3469–3476.
Hirose S, Kotani S, Uemura Y, Fujishita M, Taguchi H, Ohtsuki Y, Miyoshi I. 1988. Milk-borne transmission of human T-cell leukemia virus type I in rabbits. Virology 162:487–489.
Howard KE, Fisher IL, Dean GA, Jo Burkhard M. 2005. Methodology for isolation and phenotypic characterization of feline small intestinal leukocytes. J Immunol Methods 302:36–53.
Iwahara Y, Takehara N, Kataoka R, Sawada T, Ohtsuki Y, Nakachi H, Maehama T, Okayama T, Miyoshi I. 1990. Transmission of HTLV-I to rabbits via semen and breast milk from seropositive healthy persons. Int J Cancer 45:980–983.
Jeklova E, Leva L, Faldyna M. 2007. Lymphoid organ development in rabbits: major lymphocyte subsets. Dev Comp Immunol 31:632–644.
Jung C, Hugot JP, Barreau F. 2010. Peyer's Patches: The Immune Sensors of the Intestine. Int J Inflam 2010:823710.
Kang DW, Ohkawa S, Difabio S, Merrill KW, Fujihashi K, Yamamoto M, Miller CJ, Marthas M, McGhee JR, Eldridge JH, Murphey-Corb M, Kiyono H. 1993. Characterization of T and B cells isolated from mucosa-associated tissues of the rhesus macaque. Cell Immunol 151:379–391.
Kararli TT. 1995. Comparison of the gastrointestinal anatomy, physiology, and biochemistry of humans and commonly used laboratory animals. Biopharm Drug Dispos 16:351–380.
Kataoka R, Takehara N, Iwahara Y, Sawada T, Ohtsuki Y, Dawei Y, Hoshino H, Miyoshi I. 1990. Transmission of HTLV-I by blood transfusion and its prevention by passive immunization in rabbits. Blood 76:1657–1661.
Kimata JT, Wong FH, Wang JJ, Ratner L. 1994. Construction and characterization of infectious human T-cell leukemia virus type 1 molecular clones. Virology 204:656–664.
Kohles M. 2014. Gastrointestinal anatomy and physiology of select exotic companion mammals. Vet Clin North Am Exot Anim Pract 17:165–178.
Kotani S, Yoshimoto S, Yamato K, Fujishita M, Yamashita M, Ohtsuki Y, Taguchi H, Miyoshi I. 1986. Serial transmission of human T-cell leukemia virus type I by blood transfusion in rabbits and its prevention by use of X-irradiated stored blood. Int J Cancer 37:843–847.
Lairmore MD, Silverman L, Ratner L. 2005. Animal models for human T-lymphotropic virus type 1 (HTLV-1) infection and transformation. Oncogene 24:6005–6015.
Lal RB, Rudolph DL, Palker TJ, Coligan JE, Folks TM. 1991. A synthetic peptide elicits antibodies reactive with the external glycoprotein of human T cell lymphotropic virus type I. J Gen Virol 72(Pt 9):2321–2324.
Lefrancois L, Parker CM, Olson S, Muller W, Wagner N, Schon MP, Puddington L. 1999. The role of beta7 integrins in CD8T cell trafficking during an antiviral immune response. J Exp Med 189:1631–1638.
Lelouard H, Sahuquet A, Reggio H, Montcourrier P. 2001. Rabbit M cells and dome enterocytes are distinct cell lineages. J Cell Sci 114(Pt 11):2077–2083.
Manabe YC, Kesavan AK, Lopez-Molina J, Hatem CL, Brooks M, Fujiwara R, Hochstein K, Pitt ML, Tufariello J, Chan J, McMurray DN, Bishai WR, Dannenberg AM Jr, Mendez S. 2008. The aerosol rabbit model of TB latency, reactivation

and immune reconstitution inflammatory syndrome. Tuberculosis (Edinb) 88:187–196.

Miller H, Zhang J, Kuolee R, Patel GB, Chen W. 2007. Intestinal M cells: The fallible sentinels? World J Gastroenterol 13: 1477–1486.

Miyoshi I, Yoshimoto S, Kubonishi I, Fujishita M, Ohtsuki Y, Yamashita M, Yamato K, Hirose S, Taguchi H, Niiya K. 1985. Infectious transmission of human T-cell leukemia virus to rabbits. Int J Cancer 35:81–85.

Nagler-Anderson C. 2001. Man the barrier! Strategic defences in the intestinal mucosa. Nat Rev Immunol 1:59–67.

Nesburn AB, Bettahi I, Dasgupta G, Chentoufi AA, Zhang X, You S, Morishige N, Wahlert AJ, Brown DJ, Jester JV, Wechsler SL, BenMohamed L. 2007. Functional Foxp3+ CD4+ CD25(Bright+) "natural" regulatory T cells are abundant in rabbit conjunctiva and suppress virus-specific CD4+ and CD8+ effector T cells during ocular herpes infection. J Virol 81:7647–7661.

Neutra MR, Mantis NJ, Kraehenbuhl JP. 2001. Collaboration of epithelial cells with organized mucosal lymphoid tissues. Nat Immunol 2:1004–1009.

Nishikawa K, Takagi T. 1988. Comparative immunobiology of the palatine tonsil. Acta Otolaryngol Suppl 454:43–47.

Okita M, Mori T, Shin YS, Miyasaka M, Yamanouchi K, Mikami T, Kai C. 1995. Immunohistochemical studies of lymphoid tissues of rabbits infected with rinderpest virus. J Comp Pathol 112:41–51.

Pospisil R, Mage RG. 1998. Rabbit appendix: A site of development and selection of the B cell repertoire. Curr Top Microbiol Immunol 229:59–70.

Robek MD, Wong FH, Ratner L. 1998. Human T-cell leukemia virus type 1 pX-I and pX-II open reading frames are dispensable for the immortalization of primary lymphocytes. J Virol 72:4458–4462.

Rumbo M, Anderle P, Didierlaurent A, Sierro F, Debard N, Sirard JC, Finke D, Kraehenbuhl JP. 2004. How the gut links innate and adaptive immunity. Ann N Y Acad Sci 1029: 16–21.

Silverman LR, Phipps AJ, Montgomery A, Fernandez S, Tsukahara T, Ratner L, Lairmore MD. 2005. In vivo analysis of replication and immunogenicity of proviral clones of human T-lymphotropic virus type 1 with selective envelope surface-unit mutations. Blood 106:3602–3608.

Silverman LR, Phipps AJ, Montgomery A, Ratner L, Lairmore MD. 2004. Human T-lymphotropic virus type 1 open reading frame ii encoded p30ii is required for in vivo replication: Evidence of in vivo reversion. J Virol 78:3837–3845.

Snipes RL. 1978. Anatomy of the rabbit cecum. Anat Embryol (Berl) 155:57–80.

Tanaka Y, Tanaka R, Terada E, Koyanagi Y, Miyano-Kurosaki N, Yamamoto N, Baba E, Nakamura M, Shida H. 1994. Induction of antibody responses that neutralize human T-cell leukemia virus type I infection in vitro and in vivo by peptide immunization. J Virol 68:6323–6331.

Tanaka Y, Zeng L, Shiraki H, Shida H, Tozawa H. 1991. Identification of a neutralization epitope on the envelope gp46 antigen of human T cell leukemia virus type I and induction of neutralizing antibody by peptide immunization. J Immunol 147:354–360.

Tokarz-Deptula B, Deptula W. 2003. Dynamic alterations in peripheral blood lymphocytes in rabbits experimentally infected with VHD (viral hemorrhagic disease) virus—Polish strain Kr-1. Pol J Vet Sci 6(3 Suppl):67–69.

Tokarz-Deptula B, Deptula W. 2005. Values of selected immune and haematological parameters in healthy rabbits. Pol J Vet Sci 8:107–112.

Uemura Y, Kotani S, Yoshimoto S, Fujishita M, Yamashita M, Ohtsuki Y, Taguchi H, Miyoshi I. 1987. Mother-to-offspring transmission of human T cell leukemia virus type I in rabbits. Blood 69:1255–1258.

Uemura Y, Kotani S, Yoshimoto S, Fujishita M, Yano S, Ohtsuki Y, Miyoshi I. 1986. Oral transmission of human T-cell leukemia virus type I in the rabbit. Jpn J Cancer Res 77:970–973.

Zhao TM, Robinson MA, Bowers FS, Kindt TJ. 1995. Characterization of an infectious molecular clone of human T-cell leukemia virus type I. J Virol 69:2024–2030.